



HAL
open science

Zoledronic acid potentiates mTOR inhibition and abolishes the resistance of osteosarcoma cells to RAD001 (Everolimus): pivotal role of the prenylation process.

Gatien Moriceau, Benjamin Ory, Laura Mitrofan, Chiara Riganti, Frédéric Blanchard, Régis Brion, Céline Charrier, Séverine Battaglia, Paul Pilet, Marc G. Denis, et al.

► **To cite this version:**

Gatien Moriceau, Benjamin Ory, Laura Mitrofan, Chiara Riganti, Frédéric Blanchard, et al.. Zoledronic acid potentiates mTOR inhibition and abolishes the resistance of osteosarcoma cells to RAD001 (Everolimus): pivotal role of the prenylation process.: Additive effect of ZOL and mTOR on osteosarcoma development. *Cancer Research*, 2010, 70 (24), pp.10329-39. 10.1158/0008-5472.CAN-10-0578 . inserm-00667504

HAL Id: inserm-00667504

<https://inserm.hal.science/inserm-00667504>

Submitted on 7 Feb 2012

HAL is a multi-disciplinary open access archive for the deposit and dissemination of scientific research documents, whether they are published or not. The documents may come from teaching and research institutions in France or abroad, or from public or private research centers.

L'archive ouverte pluridisciplinaire **HAL**, est destinée au dépôt et à la diffusion de documents scientifiques de niveau recherche, publiés ou non, émanant des établissements d'enseignement et de recherche français ou étrangers, des laboratoires publics ou privés.

Zoledronic acid potentiates mTOR inhibition and abolishes the resistance of osteosarcoma cells to RAD001 (Everolimus): pivotal role of the prenylation process

Gatien Moriceau^{a, b}, Benjamin Ory^{a, b, c}, Laura Mitrofan^d, Chiara Riganti^e, Frédéric Blanchard^{a, b}, Régis Brion^{a, b}, Céline Charrier^{a, b}, Séverine Battaglia^{a, b}, Paul Pilet^f, Marc Denis^g, Leonard D. Shultz^h, Jukka Mönkkönen^d, Françoise Rédini^{a, b}, Dominique Heymann^{a, b, *}

^a INSERM, UMR 957, Nantes, F-44035 France

^b Université de Nantes, Nantes atlantique universités, Physiopathologie de la Résorption Osseuse et Thérapie des Tumeurs Osseuses Primitives

^c Massachusetts General Hospital Cancer Center and Harvard Medical School, Boston, USA

^d Department of Pharmaceutics, University of Kuopio, Finland

^e Department of Genetics, Biology and Biochemistry, University of Turin, Italy

^f INSERM, UMR 791, Nantes

^g INSERM, UMR 913, Nantes

^h The Jackson Laboratory, Bar Harbor, ME, USA

***Corresponding author:** dominique.heyman@univ-nantes.fr

Running title: Additive effect of ZOL and mTOR on osteosarcoma development

Key words: osteosarcoma, mTOR, rapamycin, bisphosphonate, drug resistance

Abstract

Despite recent improvements in therapeutic management of osteosarcoma, ongoing challenges in improving the response to chemotherapy warrants new strategies still needed to improve overall patient survival. In this study, we investigated *vivo* the effects of RAD001 (Everolimus®), a new orally available mTOR inhibitor, on the growth of human and mouse osteosarcoma cells either alone and in combination with zoledronate (ZOL), an osteoporosis drug which is used to treat bone metastases. RAD001 inhibited osteosarcoma cell proliferation in a dose- and time-dependent manner with no modification of cell cycle distribution. Combination with ZOL augmented this inhibition of cell proliferation, decreasing PI3K/mTOR signaling compared to single treatments. Notably, in contrast to RAD001, ZOL downregulated isoprenylated membrane-bound Ras concomitantly to an increase of non-isoprenylated cytosolic Ras in sensitive- and resistant-osteosarcoma cell lines to both drugs. Moreover, ZOL and RAD001 synergized to decrease Ras isoprenylation and GTP-bound Ras levels. Further, the drug combination reduced tumor development in two murine models of osteoblastic or osteolytic osteosarcoma. We found that ZOL could reverse RAD001 resistance in osteosarcoma, limiting osteosarcoma cell growth in combination with RAD001. Our findings rationalize further study of the applications of mTOR and mevalonate pathway inhibitors that can limit protein prenylation pathways.

Introduction

Current therapeutic strategies of osteosarcoma are based on tumor resection associated with highly toxic chemotherapy and fail to improve prognosis (1, 2) due to an absence of response to anti-tumor drugs observed in many cases. Failure of anti-cancer therapies often occurs from innate or/and acquired drug resistances of tumor cells to chemotherapies (3). In this context, therapies based on combinatorial drug approaches (4) appear as adapted clinical strategies for improving therapy and overcoming the multi-faceted characteristics of cancer cells.

Osteoclasts are the main target in bone of nitrogen-containing bisphosphonates (N-BP) including such as ZOL on which they induce apoptosis by inhibiting enzymes of the mevalonate pathway (5-7). Thus, the most common clinical application is osteoporosis, but bisphosphonate application has been extended to the treatment of malignant hypercalcemia. In addition, recent *in vitro* studies demonstrated an anti-tumor activity exerted by ZOL on cancer cells (8-10). Result of *in vivo* experiments also highlighted the therapeutic interest of ZOL alone or in combination with conventional chemotherapy on the growth of carcinoma (11) and sarcoma (12).

mTOR plays a key role in regulating protein metabolism, and dysregulations in mTOR signaling are frequently associated with cancer progression (13). Indeed, mTOR is a member of the PI3K family such as ATM and ATR proteins involved in DNA repair (14). mTOR functions encompass in two signaling complexes, mTORC-1 and -2, which are sensitive to rapamycin at very different concentrations (15). Thus, mTOR inhibition revealed its impact on cellular function and cell growth (16-19). Rapamycin and its analogues (RAD001, CCI-779, AP23573) (13) have shown promise in preclinical models and in clinical trials including patients suffering from neoplastic diseases (20-26). Houghton et al reported that rapamycin extends anti-tumor activity in paediatrics tumors *in vitro* and *in vivo* including osteosarcoma (27, 28). In this context, a phase II clinical trial in patients with advanced soft tissue or bone sarcomas revealed that

AP23573 exhibits single-agent activity in patients as shown by the prolonged overall survival (29) pointing out the pivotal role of the mTOR pathway in the pathogenesis of osteosarcoma. However, resistance to rapamycin has been identified and was associated with a decreased binding to it, altered mTOR up- or down-stream signaling or feedback loop associated with mTOR pathway (30).

Because RAD001 appears to be a promising agent for the treatment of neoplastic diseases, the effects of RAD001 was investigated on the growth of osteosarcoma cells, both alone and in combination with ZOL. We also investigated the mechanisms involved in the RAD001-sensitivity and resistance of osteosarcoma cells and assessed a method to abolish RAD001 resistance *in vitro* and *in vivo*.

Materials and Methods

The rat osteosarcoma OSRGA cell line established from a radio-induced osteosarcoma (31) and human MG63 cells purchased from ATCC (Promochem, France) were cultured in DMEM (Lonza, Belgium) supplemented with 10% FCS (Hyclone, USA). Murine osteosarcoma POS-1 and MOS-J cells derived from mouse spontaneous osteosarcoma were provided respectively by Dr Kamijo (32) and by Dr Shultz (33) and were cultured in RPMI with 10% FCS. Cells expressed osteoblastic markers more specifically *cbfa1/Runx2* and bone alkaline phosphatase (data not shown) and MOS-J cells are able to form mineralized nodules *in vitro* (33). These parameters were tested before cell implantation.

Cell Growth and viability

Cell growth and viability were determined by XTT reagent assay kit (Roche Molecular Biomedicals, Germany). Two thousand cells were cultured for 72 h in the presence or absence of RAD001 (0.1-100 nM), ZOL (0.1-100 μ M) or in combination of 1 or 10 nM RAD001 with 1 μ M ZOL. ZOL and RAD001 were provided by Pharma Novartis AG (Switzerland). Similar experiments were performed in the presence or absence of Clodronate (100-300 μ M, Sigma), Risedronate (2-100 μ M, Procter&Gamble, USA) or Manumycin A (2 or 3 μ M, Sigma) combined or not with 1 nM RAD001. After the culture period and addition of XTT reagent, the absorbance was then determined at 490 nm. Cell viability was also assessed by Trypan blue exclusion, viable and non-viable cells were manually counted.

Caspase Activity

Twenty thousand cells were treated for 72 h with or without RAD001 (0.1-100 nM), ZOL (0.1-100 μ M) or a combination of 1 or 10 nM RAD001 with 1 μ M ZOL. Caspase-3 activity was

assessed on 10 μ l of total cell lysates using the kit CaspACE Assay System (Promega, USA), following the manufacturer's recommendations. Results were expressed in arbitrary units and corrected for protein content quantified using the BCA test (Pierce Chemical Co.). Cells treated with 100 nM Staurosporin for 24 h were used as a positive control.

Time-lapse microscopy

Cells were cultured at 5×10^3 cells/mm² in the presence or absence of 10 nM RAD001. Time-lapse experiments were started just after adding the pharmaceutical agent. Phase-contrast photos were taken every 10 min for 72 h through a Leica DMI 6000B microscope (Germany) using X10 objective. Cell divisions in each field of observation were then manually scored in a time-dependent manner. Each condition was performed twice in duplicate.

Cell cycle Analysis

Sub-confluent OSRGA, MG63, POS-1 or MOS-J cells were incubated with or without 1 μ M ZOL and/or 1-10 nM of RAD001 for 24 h to 72 h. After the treatment period, trypsinized cells were incubated in PBS containing 0.12% Triton X-100, 0.12 mmol/L EDTA, and 100 μ g/mL DNase-free RNase A (Sigma). Then, 50 μ g/ml propidium iodide were added for 20 min at 4°C in the dark. Cell cycle distribution was studied by flow cytometry (Cytomics FC500, Beckman Coulter, France), based on 2N and 4N DNA content, and analyzed by DNA Cell Cycle Analysis Software (Phoenix Flow System, USA).

Cell signaling analysis

Two hundred thousand cells were treated with 1 μ M ZOL or/and 1-10 nM RAD001 for 72 h and then lysed in radioimmunoprecipitation (RIPA) buffer (150 mM NaCl, 5% Tris, pH 7.4, 1% NP-

40, 0.25% sodium deoxycholate, 1mM Na₃VO₄, 0.5 mM PMSF, 10 mg/ml leupeptin, 10 mg/ml aprotinin). Lysates were cleared of debris by centrifugation at 12,000 g for 15 min. Twenty microgram of total cell lysate, determined by the BCA kit, were run on 10% SDS-PAGE and electrophoretically transferred to Immobilon-P membranes (Millipore, USA). The membrane was blotted with antibodies to p-mTOR, p-p70S6K, p-4E-BP1, p-AKT, p-PI3K, p-PTEN, actin (supplemental data 1) in PBS, 0.05% Tween 20, and 3% BSA. Similarly, an unprenylated form of Rap1A was detected by western blot to indirectly quantified farnesyl di-phosphate synthase (FPPS) activity (10). The membrane was washed and probed with the secondary antibody coupled to horseradish peroxidase. Antibody binding was visualized with the enhanced chemiluminescence system (Roche Molecular Biomedicals). For quantification, the emitted glow was acquired with a CCD camera and analysed with the GeneTools program (Syngene, UK).

Ras isoprenylation and GTP-binding activity

To measure isoprenylated membrane-bound Ras and non-isoprenylated cytosolic Ras, cells were lysed in 1 ml of lysis buffer (50 mM Hepes, 750 mM KCl, 200 mM sucrose, 10 mM NaHCO₃, pH 7.4), supplemented with: protease inhibitor cocktail set III (100 mM AEBSF, 80 mM aprotinin, 5 mM bestatin, 1.5 mM E-64, 2 mM leupeptin and 1 mM pepstatin; Calbiochem, USA), 1 mM NaVO₄, 1 mM NaF, 1 mM 4-(2-Aminoethyl) benzenesulphonyl fluoride (PMSF), 10 mM aprotinin and 10 mM dithiothreitol), then sonicated (Labsonic sonicator; Germany) and centrifuged at 13,000 x g for 5 min at 4°C. Supernatants were collected and centrifuged at 100,000 x g for 1 h at 4°C; the cytosolic fraction contained in the new supernatants were collected, whereas the pellets (membrane fraction) were re-suspended in 100 µl of lysis buffer. Thirty microgram of cytosolic fraction and 60 µg of membrane fraction were subjected to 15% SDS-PAGE and western blot analysis, using an anti-Ras antibody (supplemental data 1). The

Ras-GTP binding assay was performed as previously described (34). Briefly, cells were lysed in MLB buffer (125 mM Tris-HCl, pH 7.4, 750 mM NaCl, 1% NP40, 10% glycerol, 50 mM MgCl₂, 5 mM EDTA, 25 mM NaF, 1 mM NaVO₄, 10 µg/ml leupeptin, 10 µg/ml pepstatin, 10 µg/ml aprotinin and 1 mM PMSF) and centrifuged at 13,000 x g for 10 min at 4°C. An aliquot of supernatant was taken out for determination of protein content (BCA kit). 30 µg of cell lysate were incubated for 45 min at 4°C with the Ras Assay Reagent (Raf-1 RBD, GST-tagged Agarose beads, Millipore), then the beads were washed and re-suspended in 20 µl Laemmli buffer (125 mM Tris, 4% w/v SDS, 20% v/v glycerol and 1% β-mercaptoethanol). The amount of active GTP-bound Ras was detected by SDS-PAGE and western blotting as reported above.

***In vivo* experiments**

Mice (Elevages Janvier, France) were housed under pathogen-free conditions at the Experimental Therapy Unit (Faculty of Medicine, Nantes) in accordance with the institutional guidelines of the French Ethical Committee and under the supervision of authorized investigators.

Osteoblastic osteosarcoma model: Four-week-old male C57BL/6J mice were anesthetized by inhalation of a combination Isoflurane/air associated with an i.m. injection of Buprenorphine (Temgésic®, Schering-Plough) before i.m. injection of 2 x 10⁶ MOS-J cells. Tumors appeared in contact with the tibia approximately 8 days later and lead to osteoblastic lesions reproducing the osteoblastic form of human osteosarcoma (33).

Osteolytic osteosarcoma model: Four-week-old male C3H/He mice were anesthetized as previously described before s.c. inoculation of POS-1 cell suspension (containing 2 x 10⁶ cells) in the hind footpad of the mice. Under these conditions, mice develop a primary tumor at the site of injection in 3 weeks that can be transplanted to mice of the same strain as a small fragment (2 x 2 x 2 mm) in close contact with the tibia. For this purpose, the periostum of the diaphysis was

opened and resected along a length of 5 mm, and the underlying bone was intact. The osteosarcoma fragment was placed contiguous to the exposed bone surface without the periostum, and the cutaneous and muscular wounds were sutured. Tumors appeared at the graft site approximately 8 days later associated with the development of pulmonary metastases in a 3-week period. The tumors that develop in contact to the femora lead to osteolytic lesions that reproduce the osteolytic form of human osteosarcoma (35).

For both models, the tumor volumes (V) were calculated from the measurement of two perpendicular diameters using a caliper according to the following formula: $V = 0.5 \times L \times S^2$, where L and S represent respectively, the largest and smallest perpendicular tumor diameters. Four groups of eight mice each were assigned as controls (placebo by oral administration and PBS injection subcutaneously twice a week), RAD001 (5 mg/kg, oral administration, twice a week), ZOL (100 μ g/kg, s.c, twice a week) and RAD001+ZOL (combined treatment with s.c 100 μ g/kg ZOL and 5 mg/kg RAD001 oral administration, twice weekly) groups. The treatment started one day after tumor cell implantation. Treatment continued until each animal showed signs of morbidity including cachexia or respiratory distress, at which point they were sacrificed by cervical dislocation. Analysis of architectural parameters was done using high-resolution X-ray micro-computed tomography (CT) (SkyScan-1072). Relative volume (BV/TV) of the tibia [total bone (cortical + trabecular) or trabecular bone] was quantified at necropsy on a 6.4 cm length area located between superior metaphysis and diaphysis. Radiographs were taken at the same time (PLANMED Sophie apparatus, Finland). Each experiment was repeated twice and only one set of experiments was shown.

Statistical analysis

Each experiment was repeated independently three times in triplicate. The mean \pm SD was calculated for all conditions and compared by ANOVA followed by Bonferroni post hoc test. Differences relative to a probability of two-tailed $p < 0.05$ were considered significant.

Results

RAD001 exerts a cytostatic activity on osteosarcoma cells and synergizes with N-BP *in vitro*

RAD001 significantly reduced MG63, OSRGA and POS-1 osteosarcoma cell number in a dose-dependent manner ($p < 0.01$) (IC₅₀: 0.5 nM, 1.26 nM and 45 nM for OSRGA, MG63 and POS-1 cells respectively) with a maximum effect at 100 nM (concentrations tested up to 1 μ M) (Fig. 1A). ZOL strongly diminished the number of MG63, OSRGA and POS-1 cells assessed in a dose-dependent manner (Fig. 1B). Manual counting of viable cells did not evidence cell death in any condition tested, as confirmed by the absence of caspase activity in (data not shown). Time-lapse microscopy revealed that 10 nM RAD001 clearly induced a marked decrease of mitosis in MG63, OSRGA and POS-1 osteosarcoma cells detectable at early times of the treatment (6-11 h) (Fig. 1C). Moreover, osteosarcoma cells treated with RAD001 were not blocked in any phase of the cell cycle, but the cancer cells passed through the different phases at a slightly inferior rate compared to the untreated control (data not shown). These data demonstrate that RAD001 therefore can be considered as a cytostatic drug for osteosarcoma.

Figure 2 clearly shows a significant additive effect between RAD001 and ZOL for MG63, OSRGA and POS-1 cells (Fig. 2A) ($p < 0.001$). In contrast to the combination RAD001 and risedronate (another N-BP), which induced similar combinatory effect on cell proliferation (Fig. 2B, $p < 0.001$), Clodronate (a non N-BP, 100-500 μ M) did not significantly modulate RAD001 activity. This combinatory effect between RAD001 and ZOL was confirmed by western blot analysis (Fig. 2C) (supplemental data 2). In contrast to treatment with 1 nM RAD001 which had no effect on the mTOR signaling pathway, 10 nM RAD001 significantly inhibited the mTOR signaling pathway in POS-1 and OSRGA cells, as revealed by a decrease of mTOR phosphorylation, but not in MG63 osteosarcoma cells (Fig. 2C). 1 μ M ZOL did not affect mTOR

signaling (Fig. 2C). Interestingly, the combination of 10 nM RAD001 and 1 μ M ZOL totally abolished P-mTOR and drastically inhibited its main downstream signaling partners, demonstrating a crosstalk between ZOL and mTOR signaling pathways in all MG63, OSRGA and POS-1 cells (Fig. 2B). Treatment of cells with 1 μ M ZOL did not alter unRAP1A expression, as did treatment with higher doses (data not shown, 10). Furthermore, the combination of RAD001 with ZOL strongly reduced P-PI3K, down-regulated the phosphorylation of PTEN in MG63, OSRGA and POS-1 cells and also altered AKT phosphorylation in POS-1 cells (Fig. 2C). Consequently, this combination dysregulated the mTOR downstream signaling and decreased the phosphorylation of 4EBP1 in the three cell lines assessed (Fig. 2C). p70S6K was decreased in MG63 and OSRGA and slightly in POS-1 cells (Fig. 2C).

Combined treatment with RAD001 and ZOL is efficient on RAD001 resistant-osteosarcoma cells *in vitro*

Mouse osteosarcoma MOS-J is totally refractory to RAD001 (up to 1 μ M tested) and ZOL (up to 10 μ M, 100 μ M being cytotoxic) (Fig. 3A). Interestingly, combination of RAD and ZOL at low doses induced a synergistic anti-proliferative effect on MOS-J cells (Fig. 3B, $p < 0.001$). The biological activity of RAD001 in MOS-J cells was demonstrated by western blot analyses. Indeed, 10 nM RAD001 decreased the phosphorylation of PI3K, PTEN, Akt, mTOR, P-4EBP1 and P-p70S6K (Fig. 3C) without any effect on MOS-J cell proliferation (Fig. 3B). Although ZOL alone did not also modulate these activities, ZOL and RAD001 exert an additive effect to strongly inhibit mTOR signaling (Fig. 3C).

Ras-prenylation is strongly decreased by the combined treatment with RAD001 and ZOL

Ras is located at the crossroads between ZOL and mTOR signaling pathways. Indeed, ZOL is a powerful inhibitor of FPPS activity implicated in the prenylation of small GTPases (7, 13), and the PI3K/mTOR pathway belongs to the downstream cascades of Ras activation. In this context, we first analyzed the effects of the ZOL and RAD001 combination on Ras isoprenylation (Fig. 4). 1 μ M ZOL induced a significant decrease of isoprenylated membrane-bound Ras and a concomitant increase of non-isoprenylated cytosolic Ras in all osteosarcoma cell lines tested, in contrast to 1 or 10 nM RAD001 which had no effect on Ras isoprenylation (Fig. 4A). The combined treatment of RAD001 with ZOL induced a marked decrease of Ras isoprenylation (Fig. 4A). Simultaneously, this combination reduced Ras bound to GTP (Fig. 4A). To determine the role of Ras activity in the additive effect of RAD001 and ZOL, the effect of Manumycin A, an inhibitor of Ras farnesylation, was assessed on osteosarcoma cell proliferation in combination with RAD001 (Fig. 4B). In all osteosarcoma cell lines tested (sensitive and resistant to RAD001), Manumycin A and RAD001 exert an additive effect in inhibiting cell proliferation thus mimicking ZOL activity (Fig. 4B, $p < 0.001$).

The combination of RAD001 and ZOL reduces the growth of osteosarcoma cells in syngeneic murine models

Preliminary dose-response experiments were carried out *in vivo* to determine the sub-optimal efficient doses of RAD001 and ZOL (data not shown). The ZOL dose (100 μ g/kg ZOL as research grade disodium salt) used in the present study is equivalent to the clinical dose of 4 mg IV every 3–4 weeks. However, even if dosing frequency of twice a week is greater, these doses are justified by the very aggressive nature of the osteosarcoma models used and the short

animal survival. Both drugs did not exert any side-effects on animal body weight loss or any toxic effects in MOS-J and POS-1 osteosarcoma models.

The *in vivo* effects of single- or combinatory treatment on tumor growth were first studied in a MOS-J osteosarcoma model, cells which are resistant to both agents *in vitro*. Doses of 5 mg/kg RAD001 or 100 µg/kg ZOL were chosen for the subsequent combination experiments because they had no significant effect alone on tumor growth, as compared to the control group (Fig. 5A,B). RAD001 and ZOL combination reduced the tumor volume compared to single treatment (Fig. 5A, $p < 0.001$). The relative tumor progression calculated between day 19 and day 31 confirmed the synergistic action between RAD001 and ZOL (Fig. 5B). Interestingly, combined treatment of RAD001 and ZOL significantly slowed down the tumor progression compared to a single treatment and to the control group (Fig. 5B). Furthermore, radiographs revealed that 100 µg/kg ZOL strongly reduced bone degradation (Fig. 5C) even if it had no effect on the tumor progression (Fig. 5A, B). Indeed, the metaphyses of long bones exhibited high bone density reflecting inhibition of bone resorption and retention of the primary spongiosa in contrast to 5 mg/kg RAD001, which had no protective effect of bone loss (Fig. 5C). The combination of RAD001 with ZOL had no additive inhibitory effect of bone resorption as compared to ZOL alone. By combining micro-CT image registration, the bone remodeling associated with osteosarcoma development has been followed and confirmed the radiographic analysis (Fig. 5D). One hundred µg/kg ZOL and 100 µg/kg ZOL + 5 mg/kg RAD001 significantly increased bone mass in contrast to 5 mg/kg RAD001 alone. This was confirmed by the quantification of relative bone volume (BV/TV). Indeed, BV/TV increased by approximately 40% in the presence of ZOL and ZOL + RAD001 compared to the control group (Fig. 5D, $p < 0.001$). RAD001 and ZOL induce additive effects on tumor development and reduce the growth of resistant-MOS-J osteoblastic osteosarcoma cells in syngeneic mice. Histological analyses demonstrated that the

residual bone mass of animals treated with the combination of 100 µg/kg ZOL and 5 mg/kg RAD001 was mainly composed of an extensive fibrosis associated with non-tumorigenic cells and with extensive necrotic foci compared to the other groups (Supplemental data 3). These non-tumorigenic cells which were non-responding cells to the treatment used and the necrotic tissue did not allow a complete *in vivo* analysis of the phosphorylation status of mTOR pharmacodynamic markers such as p70S6k and 4EBP1.

Similar experiments were carried out using an osteolytic-POS-1 osteosarcoma model (35). Five mg/kg RAD001 had no effect on POS-1 tumor growth compared to the control group (Fig. 6B). ZOL slightly but not significantly reduced the tumor volume (Fig. 6A, B) but markedly decreased bone degradation as shown by an increase of bone mineral density of the metaphysis (Fig. 6C). Contrarily, 5 mg/kg RAD001 alone had no effect on tumor-induced osteolysis, and the combination of RAD001 with ZOL had no additive inhibitory effect of bone resorption as compared to ZOL alone (Fig. 6C). Interestingly, RAD001 and ZOL in combination significantly decreased the tumor volume compared to the control, as well as to single treatments (Fig. 6A). Such combination treatment slowed down the tumor progression (Fig. 6B, $p < 0.001$). Micro-CT analysis confirmed the significant impact of ZOL on osteolysis with an increase in BV/TV (Fig. 6D). The combinatory treatment clearly improved the quality of bone tissue compared to the control group and the single treatments (Fig. 6D).

Discussion

The absence of response of patients suffering from osteosarcoma to chemotherapy and the lack of effectiveness of single-drug therapy led to the development of new therapeutic approaches. Indeed, therapy based on combinatorial drug regimens targeting different metabolic pathways would prevent the emergence of resistance phenomena and increase the effectiveness of treatment while reducing toxicity for patients (36). Dysregulation of the PI3K/mTOR pathway, mainly due to redundant autocrine pathways rather than mutations, is clearly involved in the pathogenesis of sarcomas. mTOR is a central crossroads of many signaling pathways induced by growth factors and nutritional status and this crossroad is deregulated in numerous cancer cells (36). It directly and indirectly controls many cellular events such as translation, transcription and protein stability and regulates cell growth, proliferation, survival and cell size (37). In this context, its functions have positioned mTOR as a potential target for cancer therapy and have stimulated the development of selective inhibitors of mTOR complexes (13). mTOR inhibitors have been already assessed in numerous malignancies (20) but only few data have been published on osteosarcoma.

The present work demonstrates the therapeutic interest of a rapamycin analogue, RAD001. RAD001 slowed down cell cycle phases in all osteosarcoma cell lines studied, but in absence of a cell cycle arrest or increase of cell death, this effect may be explained by the role exerted by mTOR on protein synthesis. Indeed, protein synthesis is regulated by mTOR complex 1 [composed by mTOR, Regulatory Associated Protein of mTOR (raptor) and G-protein subunit-like (G L)] which phosphorylates several substrates including ribosomal S6 kinase (S6K) and the eukaryote initiation factor 4E binding protein-1 (4EBP-1) (38). Once activated, S6K phosphorylates the ribosomal protein S6, resulting in the translation of a subset of mRNAs encoding for essential ribosome proteins, including eukaryotic initiation factor-4B (eIF4B) and

increasing translation mechanisms. Similar to other immunosuppressive and chemotherapeutic agents, adverse events related to RAD001 are frequent and lead to moderate dropout rates (39). Interestingly, the combination of RAD001 and ZOL clearly synergized to slow down cell proliferation in all osteosarcoma cells studied, with a marked down regulation of mTOR, 4EBP1 and p70S6K phosphorylation. Thus, this combination may be used to limit the side effects of high drug doses. mTOR signaling is controlled by an upstream signal including PI3K, Akt activation (directly on mTOR or indirectly *via* TSC1/TSC2 complex) and complex feedback inhibitions. Such feedback loops could explain that mTOR inhibition induces upstream receptor tyrosine kinase signaling activating Akt as observed in human breast and prostate carcinoma cells (40), and in OSRGA and MG63 osteosarcoma cells.

Unfortunately, resistance phenomena to rapamycin have been described (41). This is the case for mouse osteosarcoma cells used in the present study which are resistant to RAD001 and rapamycin (data not shown). *In vitro* experiments point out the additive effect between ZOL and RAD001 as revealed by the down-regulation of mTOR downstream signaling (4EBP1, p70S6K) in RAD001-sensitive and –resistant osteosarcoma cells. ZOL strongly affects the mechanism of prenylation of small GTPases leading to its inhibition (7, 13) (Fig. 7). Indeed, farnesyl diphosphate and geranylgeranyl di-phosphate are required for the posttranslational lipid modification (prenylation) of small GTPases (i.e. Ras, Rho, and Rac). Among small GTPases, Ras activates the PI3K/mTOR cascade and like mTOR, it plays a central role in the regulation of various cellular processes. However, Ras bound to GTP is able to interact strongly with PI3K (42, 43). In the present work, low doses of ZOL alone or combined with RAD001 decreased the isoprenylated-membrane bound form of Ras and increased the non-isoprenylated cytosolic Ras leading to the decrease of Ras bound to GTP and to the inhibition of the PI3K/mTOR signaling pathway. These data were confirmed by the use of manumycin A which mimicked ZOL activity.

, clearly evidencing the involvement of Ras (Fig. 7). However, if Ras is potentially involved in the additive activity between ZOL and RAD001, the alterations of other prenylated proteins can be excluded.

The additive effect of ZOL and RAD001 was confirmed in two different murine osteosarcoma models. Combination of ZOL with RAD001 resulted in a significant down-regulation of tumor progression associated with an increase of bone mass. However, no additive effect on bone the inhibition of bone resorption was evident in histomorphometric analysis confirming that ZOL potentiates RAD001 activity and not the contrary. ZOL also contributed to the decrease of tumor mass by inhibiting osteolysis. The interactions between tumor cells, tumor factors and the bone marrow microenvironment are crucial for the initiation and promotion of skeletal malignancies. These observations suggest a vicious cycle driving the formation of osteolytic bone tumors: tumor cells secrete soluble factors in bone (such as hormones, cytokines and growth factors), which stimulate osteoclastic bone resorption through indirect RANKL production by osteoblastic stromal cells (44). The osteosarcoma models used in the present work are very aggressive and did not allow the investigation of curative treatments using critical tumor volumes. Indeed, at the critical tumor size around 200-300 mm³, the bone erosion has been already set up especially for the POS-1 model and the therapeutic benefit could not be gained by starting the treatment later. In this context, the combined treatment with ZOL and RAD001 appears potentially interesting for patients who have been diagnosed at early stages of their disease.

Overall, these data provide new insights in the molecular crosstalk between mTOR and the mevalonate pathway and underline the therapeutic interest of multidrug treatment combining nitrogen bisphosphonate and mTOR inhibitors in osteosarcoma. The significance of this

combination opens new areas in the field of therapeutic multidrug strategies for the treatment of primary bone tumors, especially in osteosarcoma.

Funding and acknowledgements

This work was supported by a grant from Pharma Novartis (Rueil-Malmaison, France) and by a NIH Cancer Core grant CA34196.

References

1. Rosen G MM, Huvos AG, Gutierrez M, Marcove RC. Chemotherapy, en bloc resection, and prosthetic bone replacement in the treatment of osteogenic sarcoma. *Cancer* 1976;37:1–11.
2. Provisor AJ, Ettinger LJ, Nachman JB, et al. Treatment of nonmetastatic osteosarcoma of the extremity with preoperative and postoperative chemotherapy: a report from the Children's Cancer Group. *J Clin Oncol* 1997;15:76-84.
3. Kruh GD. Introduction to resistance to anticancer agents. *Oncogene* 2003;22(47):7262-4.
4. Liu WM. Enhancing the cytotoxic activity of novel targeted therapies--is there a role for a combinatorial approach? *Curr Clin Pharmacol* 2008;3:108-17.
5. Gibbs JB, Oliff A. The potential of farnesyltransferase inhibitors as cancer chemotherapeutics. *Annu Rev Pharmacol Toxicol* 1997;37:143-66.
6. Coxon FP, Helfrich MH, Van't Hof R, et al. Protein geranylgeranylation is required for osteoclast formation, function, and survival: inhibition by bisphosphonates and GGTI-298. *J Bone Miner Res* 2000;15:1467-76.
7. Heymann D, Ory B, Gouin F, Green JR, Redini F. Bisphosphonates: new therapeutic agents for the treatment of bone tumors. *Trends Mol Med* 2004;10:337-43.
8. Mackie PS, Fisher JL, Zhou H, Choong PF. Bisphosphonates regulate cell growth and gene expression in the UMR 106-01 clonal rat osteosarcoma cell line. *Br J Cancer* 2001;84:951-9.
9. Terpos E, Sezer O, Croucher PI, et al. The use of bisphosphonates in multiple myeloma: recommendations of an expert panel on behalf of the European Myeloma Network. *Ann Oncol* 2009;20:1303-17.
10. Ory B, Blanchard F, Battaglia S, Gouin F, Redini F, Heymann D. Zoledronic acid activates the DNA S-phase checkpoint and induces osteosarcoma cell death characterized by apoptosis-inducing factor and endonuclease-G translocation independently of p53 and retinoblastoma status. *Mol Pharmacol* 2007;71:333-43.
11. Ottewell PD, Monkkonen H, Jones M, Lefley DV, Coleman RE, Holen I. Antitumor effects of doxorubicin followed by zoledronic acid in a mouse model of breast cancer. *J Natl Cancer Inst* 2008;100:1167-78.
12. Heymann D, Ory B, Blanchard F, Heymann MF, Coipeau P, Charrier C, et al. Enhanced tumor regression and tissue repair when zoledronic acid is combined with ifosfamide in rat osteosarcoma. *Bone* 2005;37:74-86.

13. Ory B, Moriceau G, Redini F, Heymann D. mTOR inhibitors (rapamycin and its derivatives) and nitrogen containing bisphosphonates: bi-functional compounds for the treatment of bone tumours. *Curr Med Chem* 2007;14:1381-7.
14. Vezina C, Kudelski A, Sehgal SN. Rapamycin (AY-22,989), a new antifungal antibiotic. I. Taxonomy of the producing streptomycete and isolation of the active principle. *J Antibiot (Tokyo)* 1975;28:721-6.
15. Foster DA, Toschi A. Targeting mTOR with rapamycin: one dose does not fit all. *Cell Cycle* 2009;8:1026-9.
16. Wullschleger S, Loewith R, Hall MN. TOR signaling in growth and metabolism. *Cell* 2006, 124:471-84.
17. Reiling JH, Sabatini DM. Stress and mTOR signaling. *Oncogene* 2006;25:6373-83.
18. Petiot A, Pattingre S, Arico S, Meley D, Codogno P. Diversity of signaling controls of macroautophagy in mammalian cells. *Cell Struct Funct* 2002;27:431-41.
19. Mamane Y, Petroulakis E, LeBacquer O, Sonenberg N. mTOR, translation initiation and cancer. *Oncogene* 2006;25:6416-22.
20. MacKenzie AR, von Mehren M. Mechanisms of mammalian target of rapamycin inhibition in sarcoma: present and future. *Expert Rev Anticancer Ther* 2007;7:1145-54.
21. Khariwala SS, Kjaergaard J, Lorenz R, Van Lente F, Shu S, Strome M. Everolimus (RAD) inhibits in vivo growth of murine squamous cell carcinoma (SCC VII). *Laryngoscope* 2006;116:814-20.
22. Wan X, Mendoza A, Khanna C, Helman LJ. Rapamycin inhibits ezrin-mediated metastatic behavior in a murine model of osteosarcoma. *Cancer Res* 2005;65:2406-11.
23. Cutler C, Antin JH. Mammalian target of rapamycin inhibition as therapy for hematologic malignancies. *Cancer* 2004;101:1478.
24. Kauffman HM, Cherikh WS, Cheng Y, Hanto DW, Kahan BD. Maintenance immunosuppression with target-of-rapamycin inhibitors is associated with a reduced incidence of de novo malignancies. *Transplantation* 2005;80:883-9.
25. Reddy GK, Mughal TI, Rini BI. Current data with mammalian target of rapamycin inhibitors in advanced-stage renal cell carcinoma. *Clin Genitourin Cancer* 2006;5:110-3.
26. Haritunians T, Mori A, O'Kelly J, Luong QT, Giles FJ, Koeffler HP. Antiproliferative activity of RAD001 (everolimus) as a single agent and combined with other agents in mantle cell lymphoma. *Leukemia* 2007;21:333-9.
27. Houghton PJ, Morton CL, Kolb EA, Gorlick R, Lock R, Carol H, et al. Initial testing (stage 1) of the mTOR inhibitor rapamycin by the pediatric preclinical testing program. *Pediatr Blood Cancer* 2008;50:799-805.
28. Zhou Q, Deng Z, Zhu Y, Long H, Zhang S, Zhao J. mTOR/p70S6K signal transduction pathway contributes to osteosarcoma progression and patient's prognosis. *Med Oncol* 2009; in press.
29. Chawla SP, Tolcher AW, Staddon AP, Schuetze S, D'Amato GZ, Blay JY, Loewy J, Kan R, Demetri GD. Survival results with AP23573, a novel mTOR inhibitor, in patients with advanced soft tissue or bone sarcomas: update of phase II trial. *ASCO Annual Meeting Proceedings. J Clin Oncol* 2007;25 (18S):10076.
30. Jiang BH, Liu LZ. Role of mTOR in anticancer drug resistance: perspectives for improved drug treatment. *Drug Resist Updat* 2008;11:63-76.
31. Klein B, Pals S, Masse R, et al. Studies of bone and soft-tissue tumours induced in rats with radioactive cerium chloride. *Int J Cancer* 1977;20:112-9.

32. Kamijo A, Koshino T, Uesugi M, Nitto H, Saito T. Inhibition of lung metastasis of osteosarcoma cell line POS-1 transplanted into mice by thigh ligation. *Cancer Lett* 2002;188:213-9.
33. Joliat MJ, Umeda S, Lyons BL, Lynes MA, Shultz LD. Establishment and characterization of a new osteogenic cell line (MOS-J) from a spontaneous C57BL/6J mouse osteosarcoma. *In Vivo* 2002;16:223-8.
34. Laezza C, Fiorentino L, Pisanti S, Gazzero P, Caraglia M, Portella G, Vitale M, Bifulco M. Lovastatin induces apoptosis of k-ras-transformed thyroid cells via inhibition of ras farnesylation and by modulating redox state. *J Mol Med* 2008;86:341-51.
35. Lamoreux F, Richard P, Wittrant Y, Battaglia S, Pilet P, Trichet V, et al. Therapeutic Relevance of Osteoprotegerin Gene Therapy in Osteosarcoma: Blockade of the Vicious Cycle between Tumor Cell Proliferation and Bone Resorption. *Cancer Res* 2007;67:7308-18.
36. Bjornsti MA, Houghton PJ. The TOR pathway: a target for cancer therapy. *Nat Rev Cancer* 2004;4:335-48.
37. Fingar DC, Salama S, Tsou C, Harlow E, Blenis J. Mammalian cell size is controlled by mTOR and its downstream targets S6K1 and 4EBP1/eIF4E. *Genes Dev* 2002;16:472-87.
38. Hara K, Yonezawa K, Weng QP, Kozlowski MT, Belham C, Avruch J. Amino acid sufficiency and mTOR regulate p70 S6 kinase and eIF-4E BP1 through a common effector mechanism. *J Biol Chem* 1998;273:14484-94.
39. Sanchez-Fructuoso AI. Everolimus: an update on the mechanism of action, pharmacokinetics and recent clinical trials. *Expert Opin Drug Metab Toxicol* 2008;4:807-19.
40. O'Reilly KE, Rojo F, She QB, et al. mTOR inhibition induces upstream receptor tyrosine kinase signaling and activates Akt. *Cancer Res* 2006;66:1500-8.
41. Kim SH, Zukowski K, Novak RF. Rapamycin effects on mTOR signaling in benign, premalignant and malignant human breast epithelial cells. *Anticancer Res* 2009;29:1143-50.
42. Kiel C, Filchtinski D, Spoermer M, Schreiber G, Kalbitzer HR, Hermann C. Improved binding raf to Ras.GDP is correlated with biological activity. *J Biol Chem* 2009;284:319893-902.
43. Konstantinopoulos PA, Karamouzis MV, papavassiliou AG. Post-translational modifications and regulation of the RAS superfamily of GTPases as anticancer targets. *Nat Rev Drug Discov* 2007;6:541-55
44. Wittrant Y, Theoleyre S, Chipoy C, et al. RANKL/RANK/OPG: new therapeutic targets in bone tumours and associated osteolysis. *Biochim Biophys Acta* 2004;1704:49-57.

Figure legends

Figure 1: ZOL and RAD001 differentially affect osteosarcoma cell proliferation. Viability of osteosarcoma cells treated with RAD001 (A) or ZOL (B) for 72 h, Mean \pm SD of three independent experiments performed in triplicate. * $p < 0.05$; ** $p < 0.01$; *** $p < 0.001$ compared to the control. (C) Kinetic of cell divisions analyzed by time-lapse microscopy with or without 10 nM of RAD001.

Figure 2: ZOL and RAD001 crosstalk: ZOL potentiates the RAD001 inhibition on osteosarcoma cell proliferation. (A) Viability of osteosarcoma cells treated with 1 μ M ZOL combined or not with 1 or 10 nM RAD001 for 72h. (B) Viability of MG63 cells treated with 10 nM RAD001 combined or not with 100 μ M clodronate (Clo.) or 20 μ M risedronate (Ris.), determined by XTT assay. Graphs represent the mean \pm SD of three independent experiments performed in triplicate. *** $p < 0.001$, NS: not significant. (C) Representative blots of PI3K/mTOR signaling pathways.

Figure 3: RAD001 and ZOL exert additive effect on the proliferation of resistant-osteosarcoma cells. (A) Number of viable MOS-J cells treated by ZOL (0.1 to 100 μ M) or RAD001 (0.1 to 100 nM) or (B) a combination of both agents for 72 h. Graphs represent the mean \pm SD of three independent experiments performed in triplicate. *** $p < 0.001$. (C) Representative blots of PI3K/mTOR signaling pathways.

Figure 4: The inhibition of Ras prenylation is involved in the additive effect between RAD001 and ZOL. (A) Representative blot of isoprenylated-membrane bound Ras, non-isoprenylated cytosolic Ras and Ras bound to GTP in osteosarcoma cells treated with 1 μ M ZOL combined or not with 1 or 10 nM RAD001 for 72 h. (B) Viability of osteosarcoma cells treated for 72h with 1 nM RAD001 in the presence or absence of 2 μ M manumycin A. *** p <0.001 compared to single treatment.

Figure 5: Effect of combinatory treatment of RAD001 with ZOL on the growth of resistant-MOS-J osteosarcoma cells in syngeneic mice. Mice bearing MOS-J tumors (n=8/group) were assigned as CT (vehicle), RAD001 (5 mg/kg, twice weekly), ZOL (100 μ g/kg, twice a week) or RAD001+ZOL groups. (A) The treatment started one day after tumor cell implantation (arrow). Evolution of tumors volumes (V). (B) Follow up of tumor progressions. * p < 0.05; *** p < 0.001. (C) Radiographs taken at the time of sacrifice. (D) micro-CT analyses performed on bones explanted. Bone Volume: BV, Total Volume: TV.

Figure 6: ZOL and RAD001 induce additive inhibition of tumor growth in osteolytic POS-1 osteosarcoma model. Mice bearing POS-1 tumors (n=8/group) were assigned as CT (vehicle), RAD001 (5 mg/kg, twice weekly), ZOL (100 μ g/kg, twice weekly) or RAD001+ZOL groups. (A) The treatment started one day after tumor cell implantation (arrow). Follow up of tumor progressions. *** p < 0.001. (C) Radiographs taken at the time of sacrifice. (D) micro-CT analyses performed on explanted bones. Bone Volume: BV, Total Volume: TV.

Figure 7: Diagram summarizing the mechanism of action of ZOL and RAD001 on osteosarcoma cells and the crosstalk between mTOR and mevalonate pathways.

Fig. 1

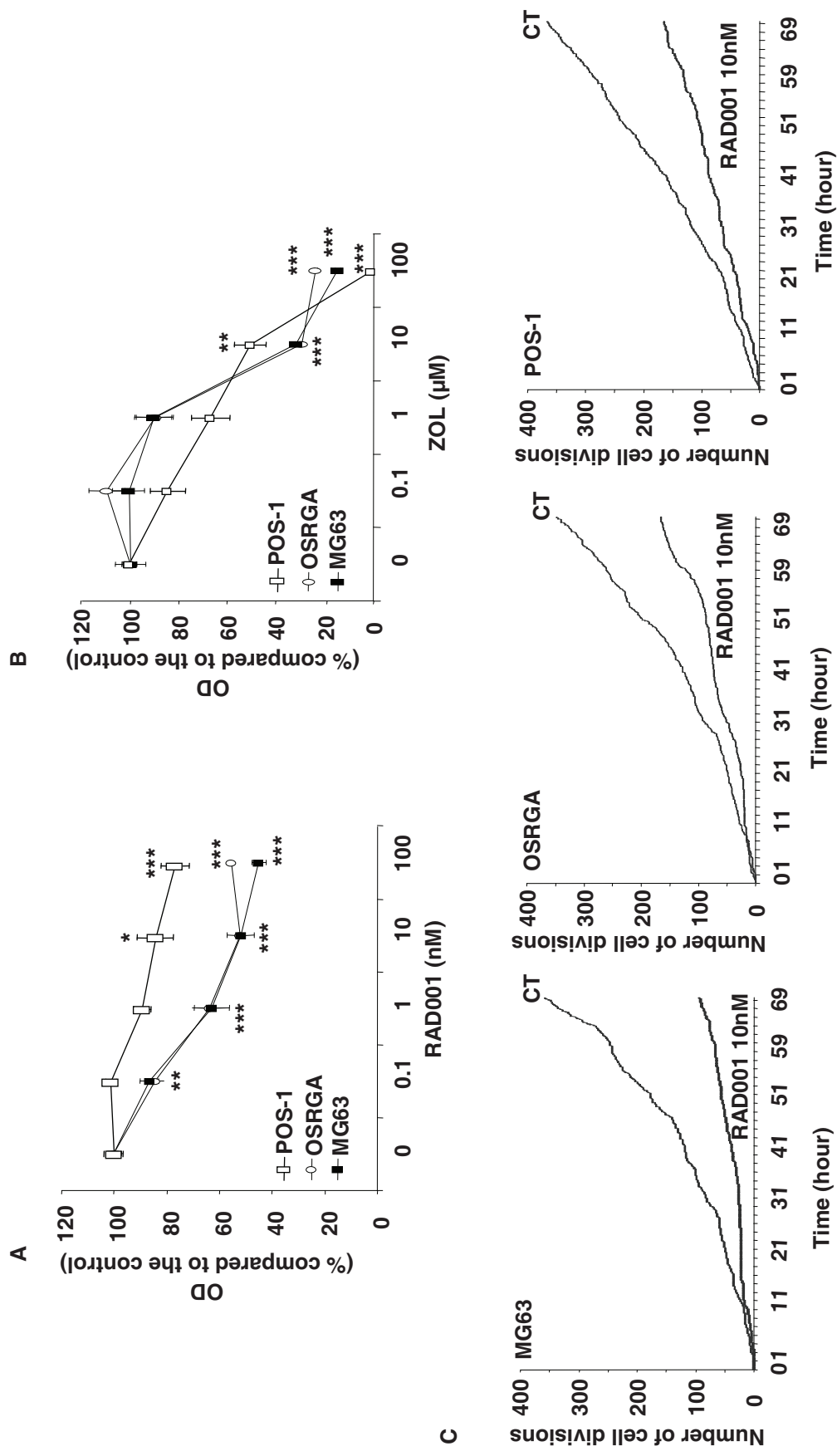


Fig.2

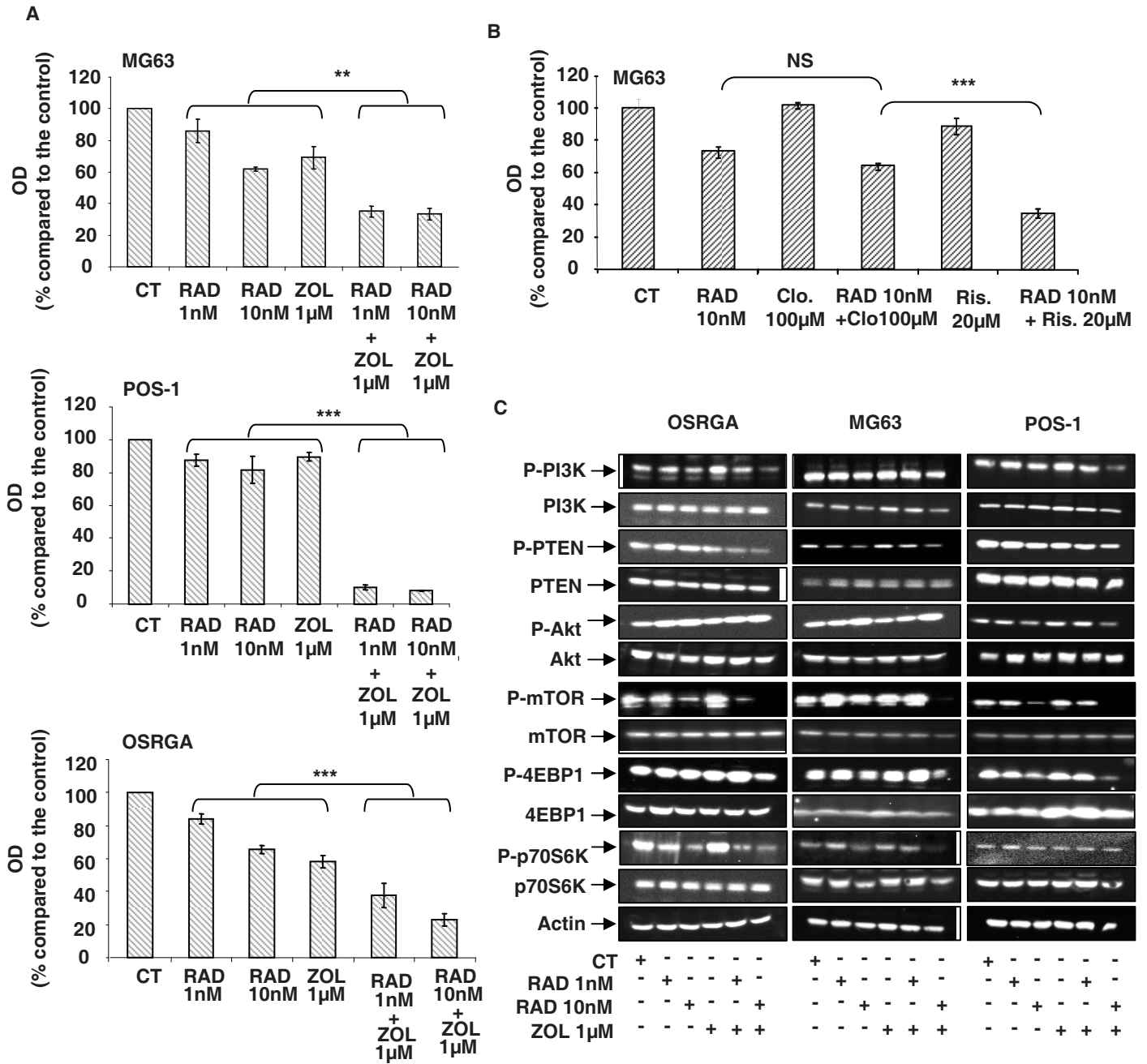


Fig. 3

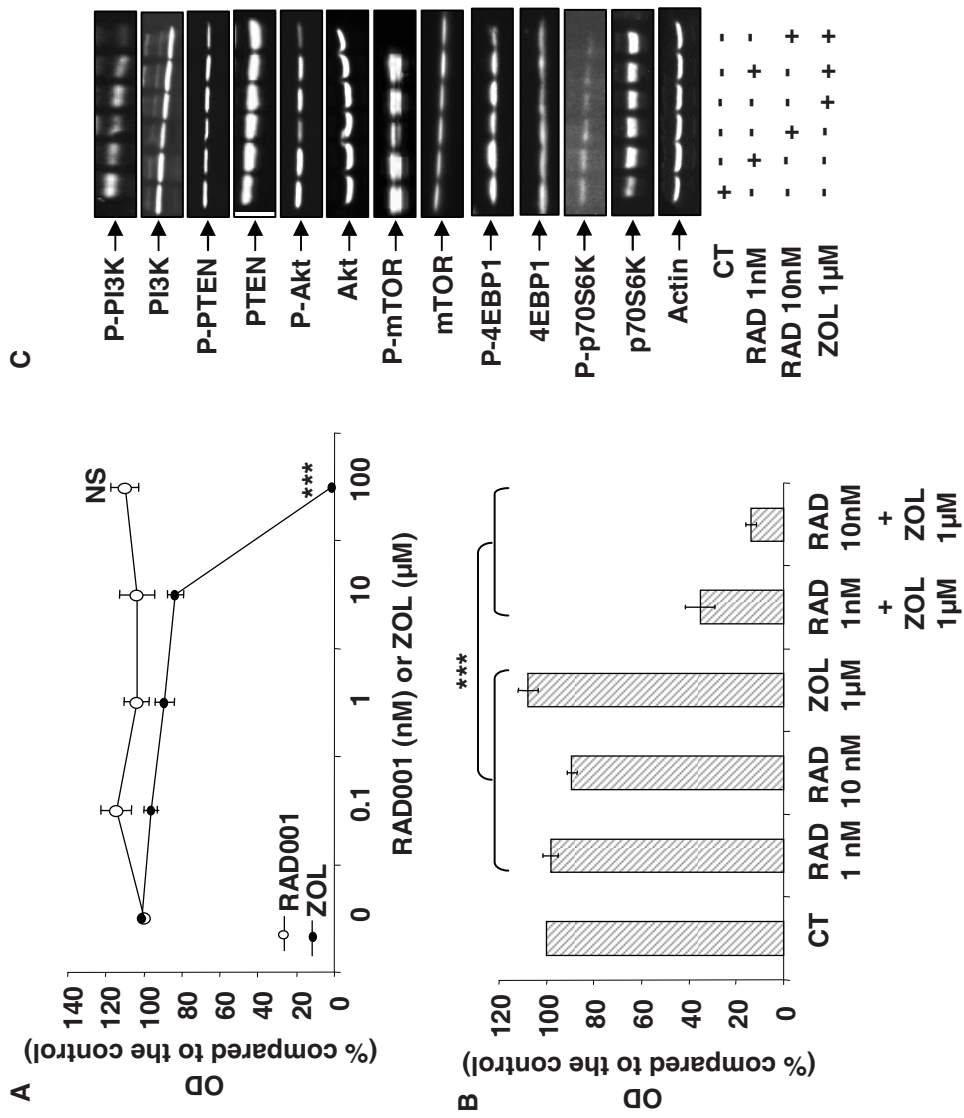
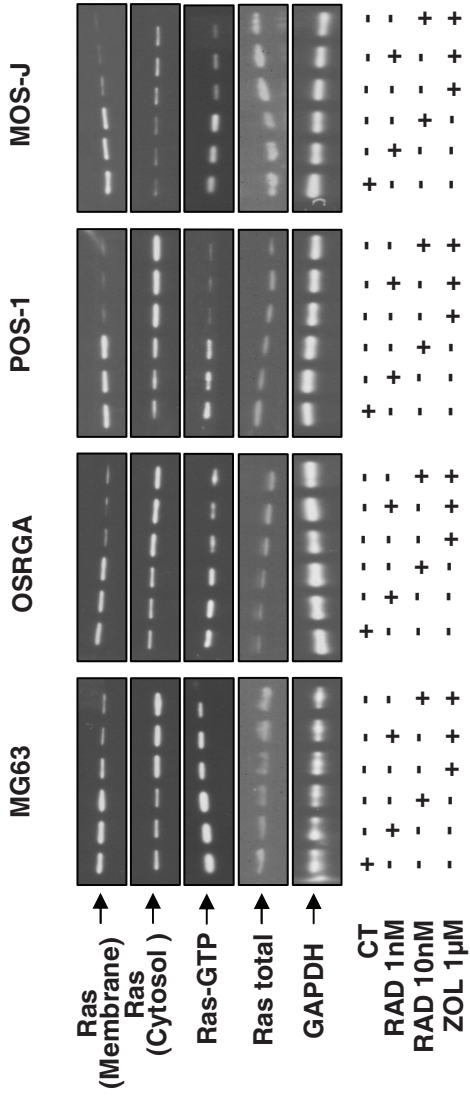


Fig.4

A



B

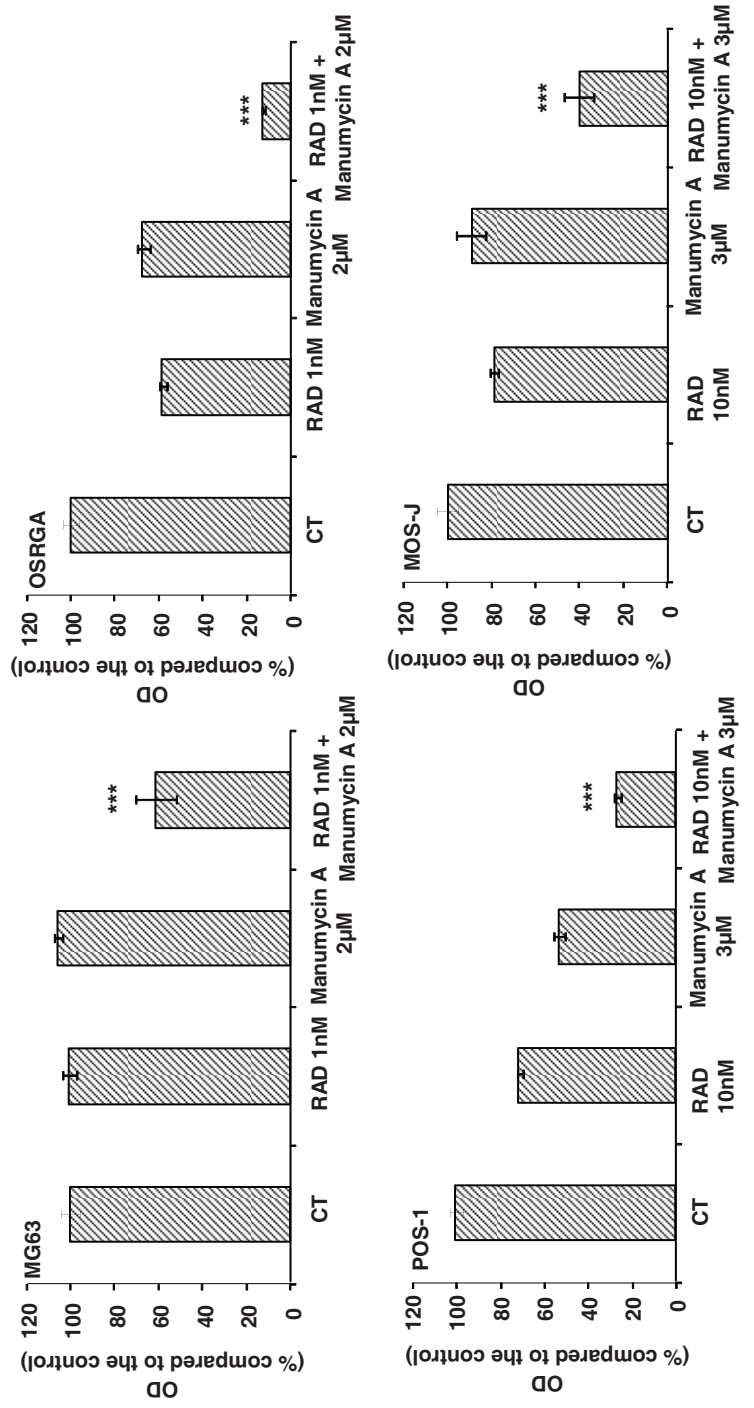


Fig. 5

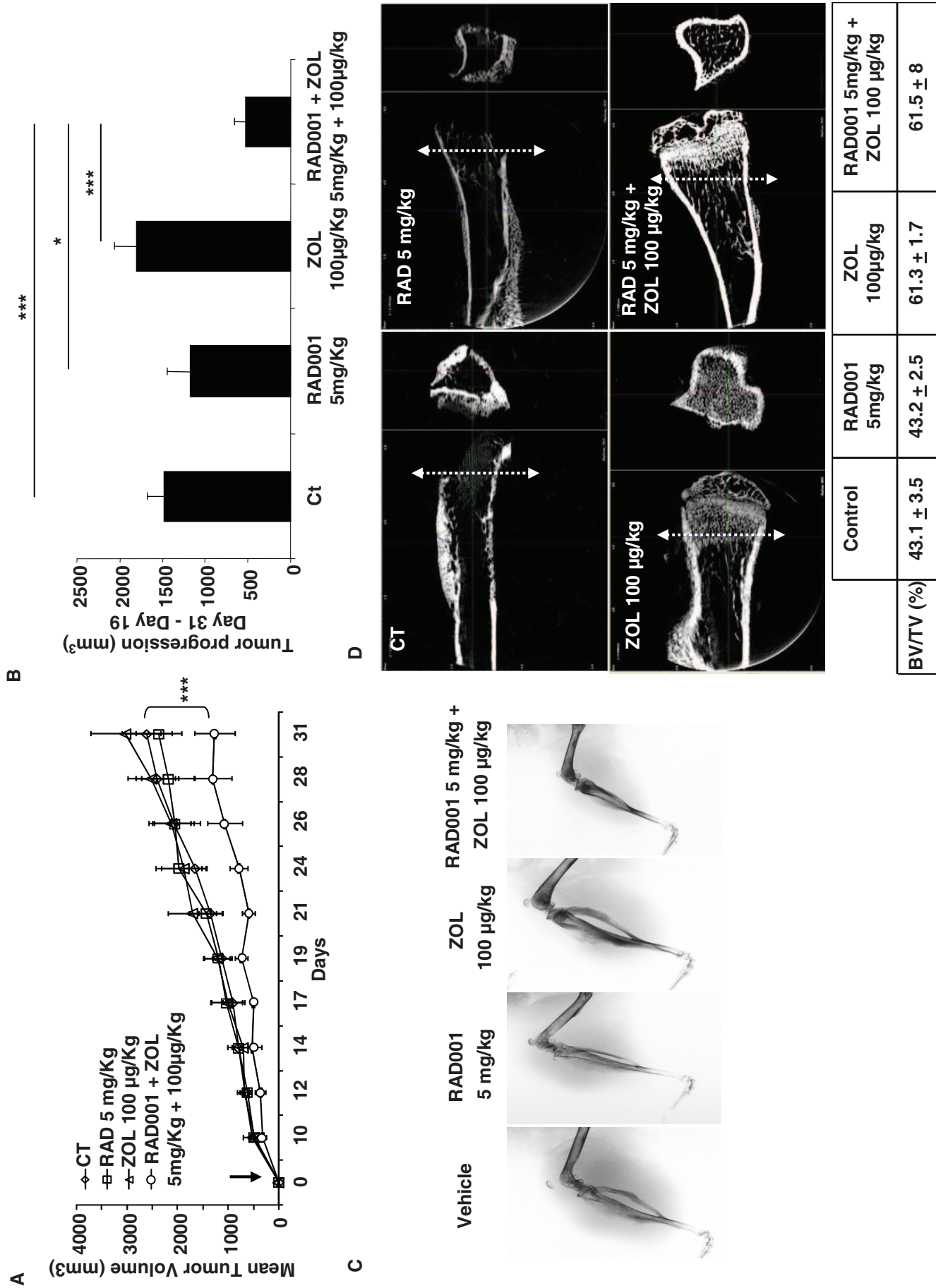


Fig. 6

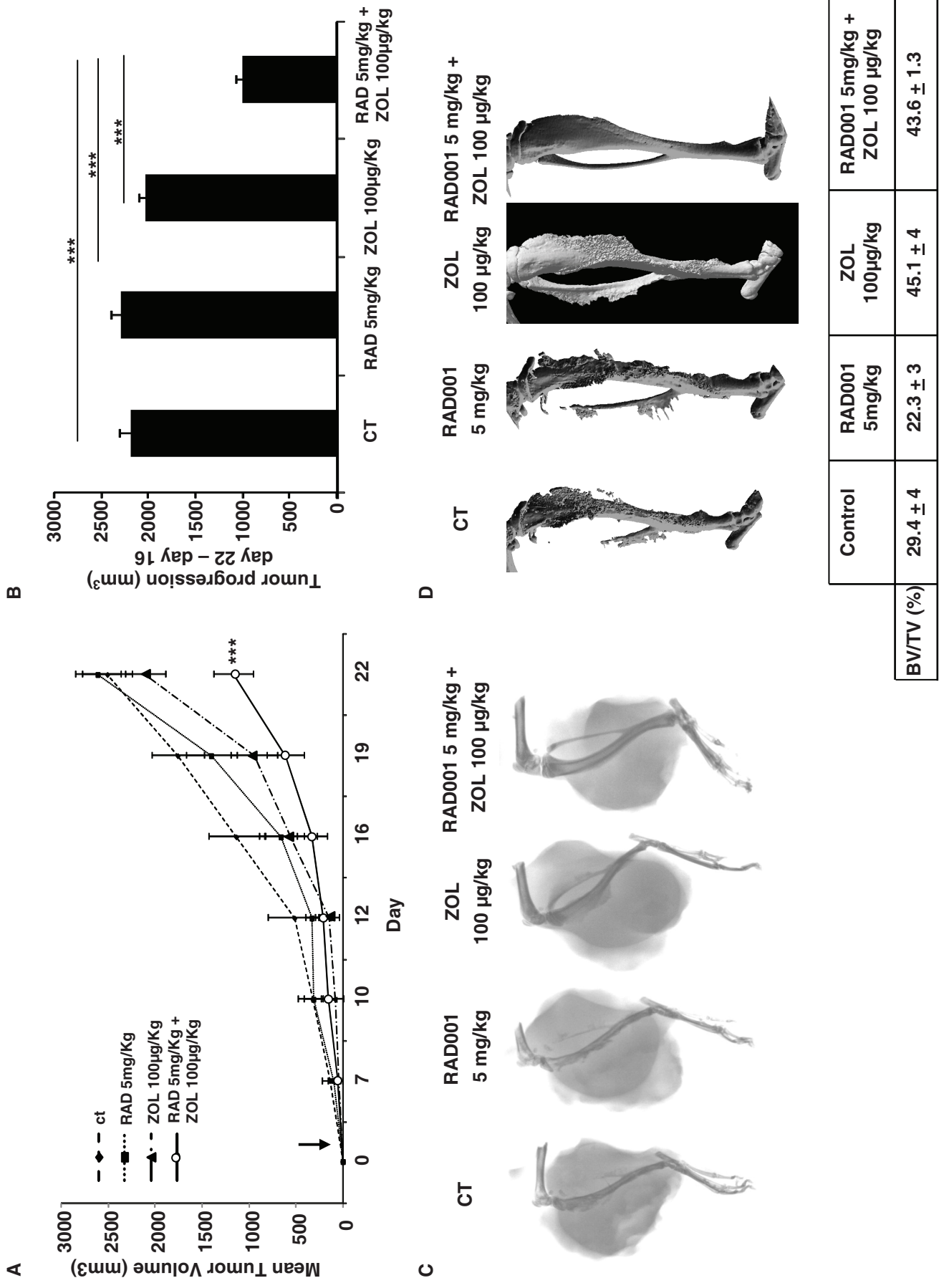


Fig.7

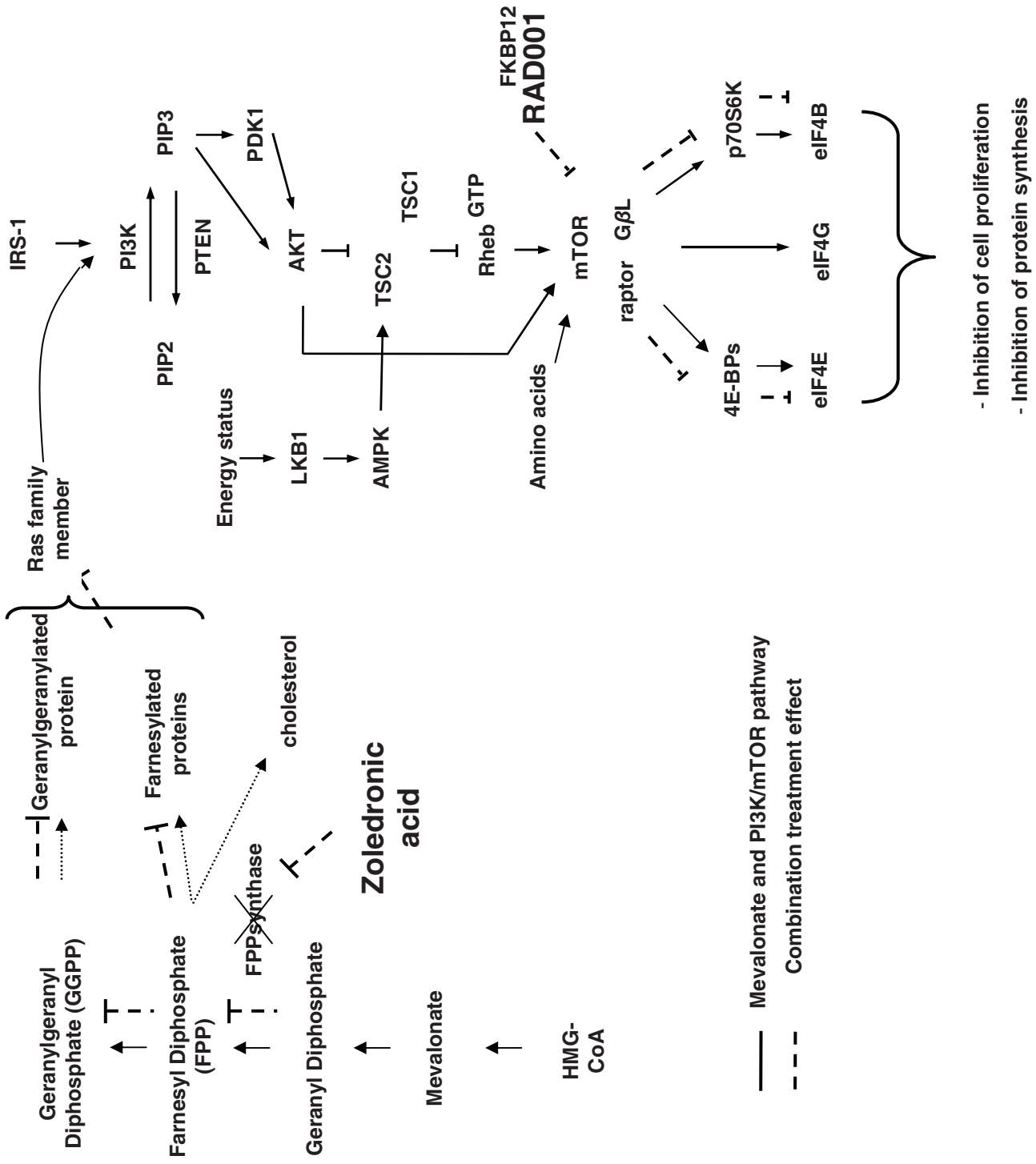
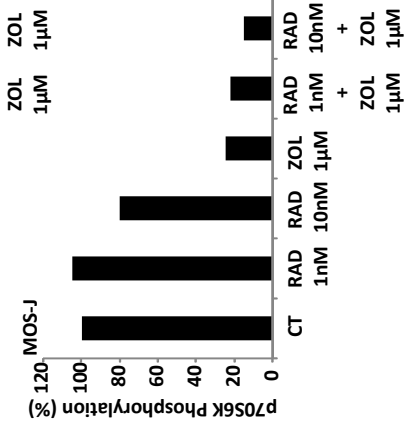
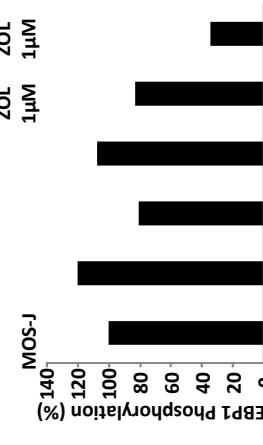
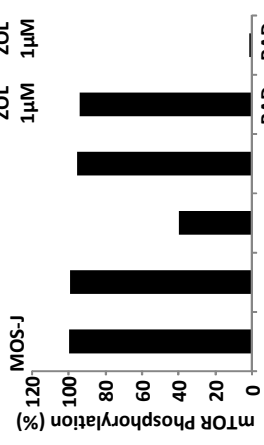
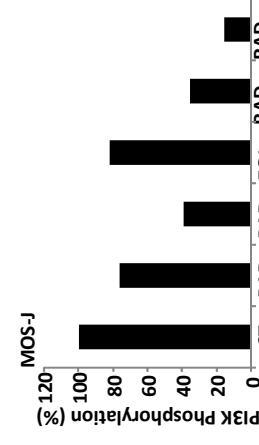
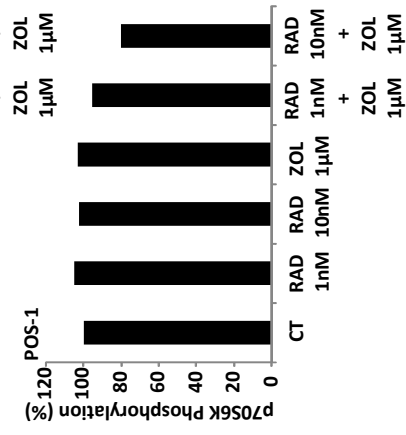
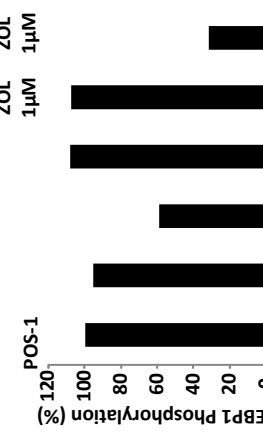
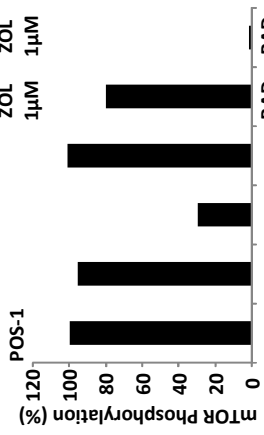
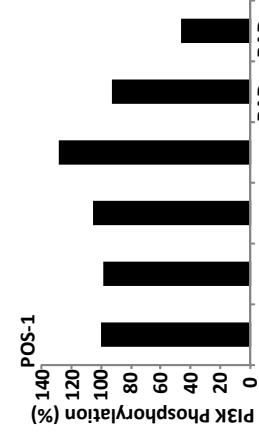
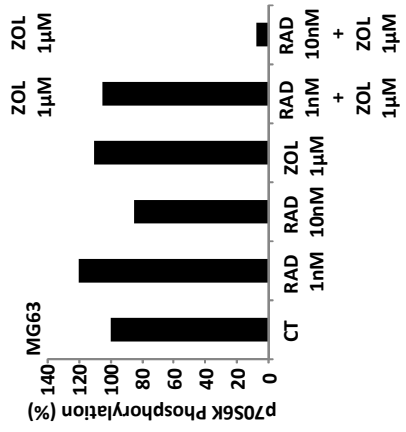
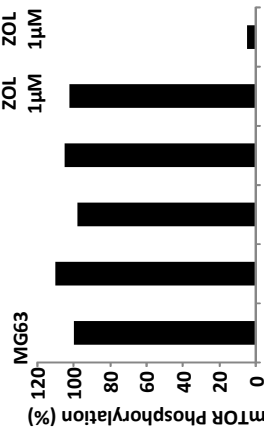
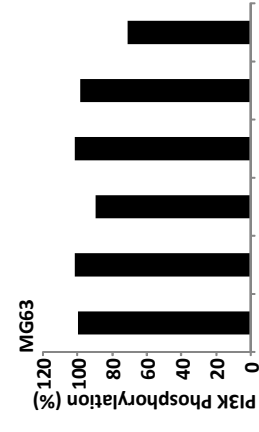
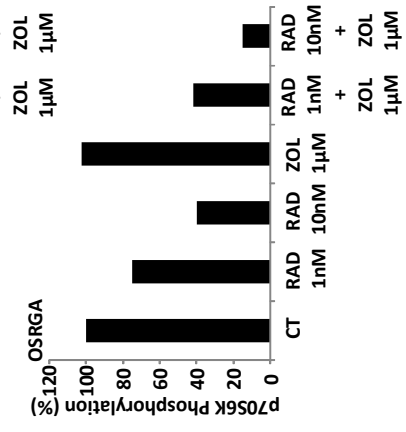
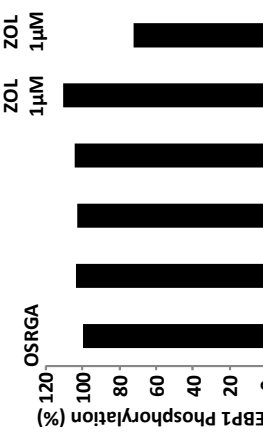
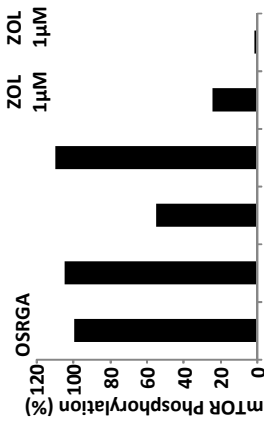
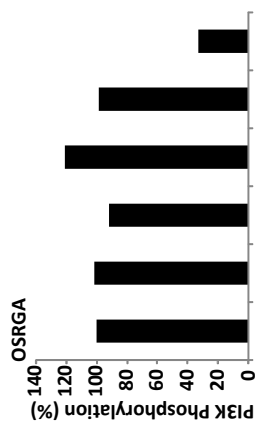
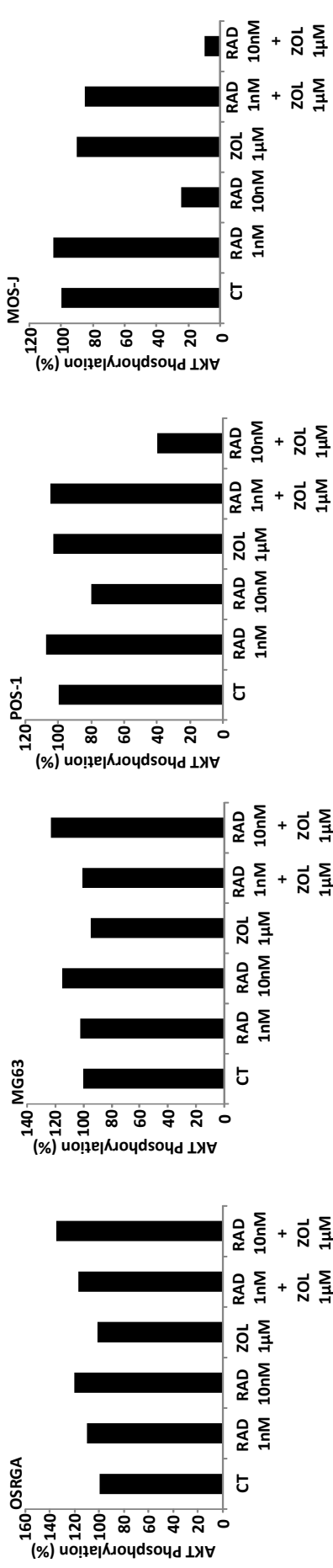
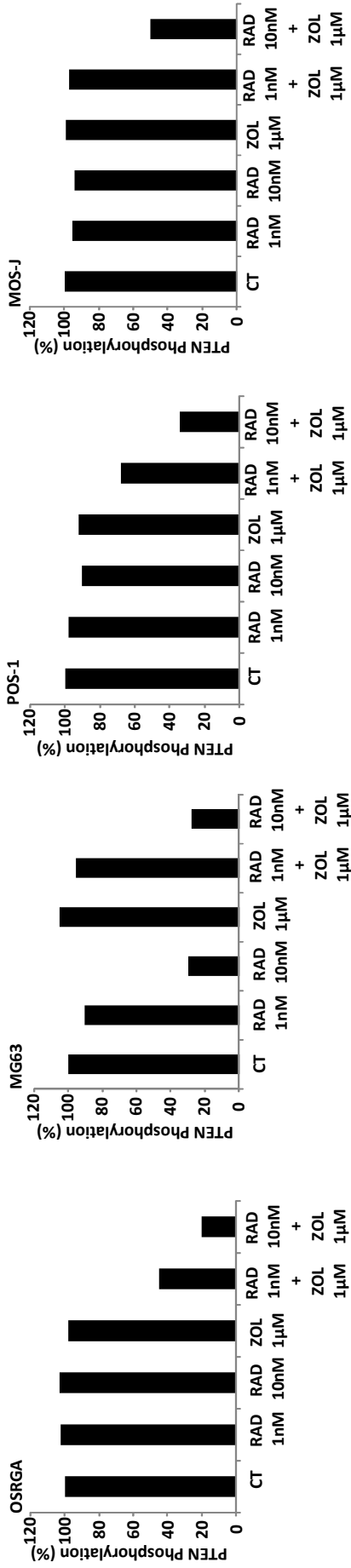


Table 1 : Primary antibodies used for cell signaling analysis

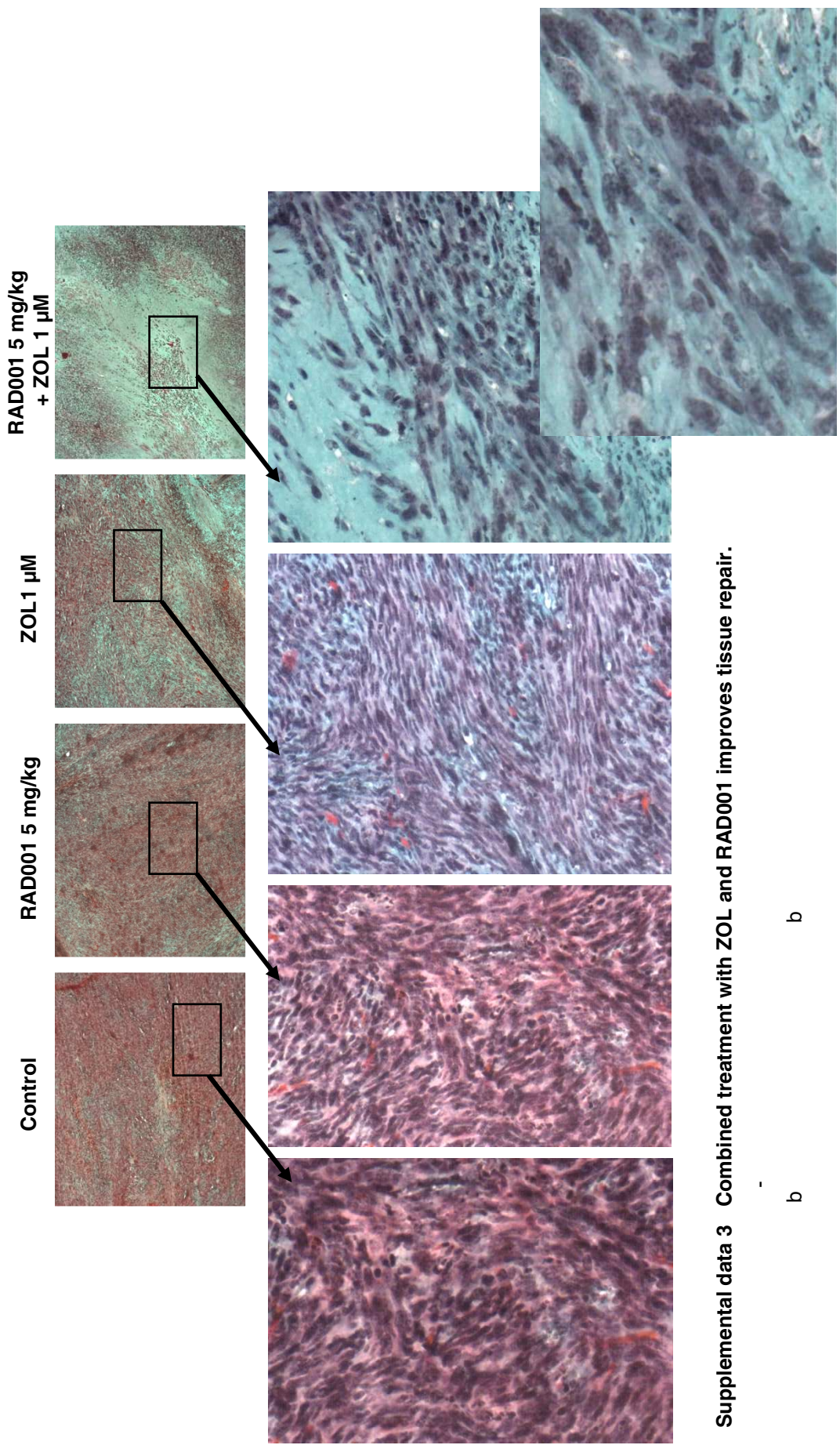
Antibodies and origin	Phosphorylated residue	Species	Dilution	Reference
Cell signalling (SA)				
P-mTOR	Ser 4228	Rabbit	1/1000	2971
mTOR		Rabbit	1/1000	2972
P-P70S6K	Thr 421/Ser424	Rabbit	1/1000	9204
P70S6K		Rabbit	1/1000	9202
P-4EBP1	Thr 70	Rabbit	1/1000	9455
4EBP1		Rabbit	1/1000	9452
P-AKT	Ser 473	Rabbit	1/1000	9271
AKT		Rabbit	1/1000	9272
P-PI3Kp85/p55	Tyr 458/Tyr 199	Rabbit	1/1000	4228
PI3K		Rabbit	1/1000	4292
P-PTEN	Ser 380	Rabbit	1/1000	9551
PTEN		Rabbit	1/1000	9552
Sigma (France)				
Actin	NA	Rabbit	1/1000	A5060
Santa Cruz (SA)				
UnRAP1A	NA	Goat	1/1000	SC 1482
Millipore (SA)				
Ras	NA	Mouse	1/1000	05-516, clone RAS10





Supplemental data 2: quantification of the intensity of the bands obtained by western blot shown in Figure 2 C

Supplemental data 3



Supplemental data 3 Combined treatment with ZOL and RAD001 improves tissue repair.

b b